Tiling model for glass formation with incremental domain-size kinetics

Thomas A. Weber and Frank H. Stillinger
AT&T Bell Laboratories, Murray Hill, New Jersey 07974
(Received 15 December 1986; revised manuscript received 17 February 1987)

The equilibrium and kinetic properties of the square-tiling model proposed by Stillinger and Weber had been studied previously by Monte Carlo simulation using a set of kinetic transition-rate rules which allowed only those aggregation and fragmentation processes which involved a minimal number of square arrays of square tiles. In the present work a new set of transition-rate rules is studied which allows fragmentation and aggregation to occur at the boundary by the shedding or addition of L-shaped arrays of unit squares. The equilibrium properties of the model at temperatures above the condensation point are found to be in excellent agreement with those found using the minimal-aggregation transition-rate rules. The kinetic properties are found to differ significantly. The current model is found to relax substantially more rapidly and to produce a somewhat different texture of tiles in the low-temperature glass. The relaxation of the potential autocorrelation function (as before) is found to be nonexponential and can be described by the Kohlrausch-Williams-Watts equation with a temperature-dependent fractional exponent. In addition the system still exhibits non-Arrhenius temperature dependence of the average relaxation rate.

I. INTRODUCTION

The thermodynamic and kinetic properties of supercooled liquids and the glasses they form show a rich diversity of phenomena including very-low-temperature anomalies, cooling-rate dependencies, nonexponential relaxation behavior, and strong hysteresis effects.[1] The quantitative details of the behavior of a material in the vicinity of its glass transition depend of course upon atomic and molecular interactions of the glass former. In an attempt to understand and explain the properties of glasses, however, theorists have responded by studying a large number of "models" some of which are purely phenomenological while others attempt to quantify the relevant atomic and molecular processes which are involved in the macroscopic observables.[2–15]

We have recently introduced a simple tiling model for glass formation which precisely identifies the energy of various states and which allows dynamical transitions between states in an ergodic manner.[16,17] Through a combination of both an analytical approach and the results from Monte Carlo simulations we were able to accurately determine the equilibrium thermodynamical properties of this model at temperatures greater than the glass transition.

In the first simulations of this tiling model, the dynamical transition rates which specify the kinetic properties of the model were chosen according to a principle of minimal aggregation or fragmentation.[17] Specifically, in the two-dimensional implementation of the model, a square tile was allowed to fragment only into the cluster of the smallest number of squares all of the same size. Thus, for example, a 6×6 square could fragment into four 3×3 squares but not into nine 2×2 squares. The reverse process occurred by allowing only those aggregations of squares which could have been produced by a single fragmentation process.

In this paper we investigate another set of dynamical transition rates for the square-tiling model, namely, boundary aggregation or fragmentation. In the present case a square is allowed to shrink into a square whose side length is one unit smaller, thereby shedding an L-shaped assemblage of unit squares. Thus, for example, a 6×6 square could fragment into a 5×5 square and 11 unit squares. The allowed aggregation processes are merely the reverse of the allowed fragmentations (shrinkages). The point of introducing this new kinetic variant is to see how sensitive low-temperature relaxations are to details of the fundamental kinetic processes allowed.

Section II defines the "tiling model" and dynamical transition rates used to specify both the minimal fragmentation and boundary shift models. Section III provides details of the Monte Carlo simulation and presents the equilibrium thermodynamic properties deduced from the simulations. The kinetic rate processes and relaxation behavior as revealed through simulations are discussed in Sec. IV. The closing section, V, summarizes the differences observed in the kinetic properties of the model due to the choice of two distinctly different sets of dynamical transition rates.

II. TILING MODELS

In previous molecular-dynamics simulations of simple liquids, we have created mechanically stable amorphous packings using a mass-weighted steepest-descent technique starting from the hot liquid.[18] These packings represent local minima of the potential energy hypersurface. It is the discrete set of these mechanically stable packings which uniquely determine the properties of the supercooled liquid or glass. For the most part the local vibrational deformations away from these potential energy minima may be disregarded at very low temperature.

A careful study of the amorphous packings produced

from these rapid quenches shows that there is substantial variability in the size and local geometry of such regions. For example, the local stress is found to be highly anisotropic due to defects in local coordination geometry and in the strength of bonding within a region.[19]

These observations provide the justification for the tiling model of glass formation. In this model the glass is characterized as an ensemble of domains of various sizes. Within the interior of a domain there are well-bonded, well-coordinated atoms or molecules. The domain boundaries themselves are the sites of local strain caused by geometric frustration. This strain may be due to bonds weakened because of steric effects or due to problems in coordination number, involving either too few or too many atoms or molecules.

The tiling model then represents the statistical mechanics of the way domains are joined together, and of the kinetics of interconversion of differing domain patterns. The following simplifying assumptions have been invoked to make the simulations of this model manageable. (a) The system is two dimensional. (b) Domains are represented as squares with integer side length. (c) All domain sizes are allowed. (d) Periodic boundary conditions apply.

The potential energy Φ of a tiling is taken to be proportional to the total length of interdomain boundary times λ, a positive energy per unit length of boundary. Therefore Φ is given by

$$\Phi = 2\lambda \sum_{j(\geq 1)} j n_j \ , \tag{2.1}$$

where n_j is the number of square domains of size $j \times j$. The total area of the system is fixed at N, which requires that the potential energy Φ of any configuration fall within the following bounds:

$$2\lambda N^{1/2} \leq \Phi \leq 2\lambda N \ . \tag{2.2}$$

A configuration consisting all of unit squares has the maximum potential energy. A configuration of one system-spanning square with area N has the minimum potential energy.

In chosing a set of dynamical transition rates for the tiling model, two properties must be considered. Firstly, the rates must be consistent with ergodic behavior, which means that any configuration must be accessible from any other by a finite set of transitions. Secondly, the allowed transitions must be sufficiently sparse so that system configurations manifest glasslike behavior on cooling to low temperature rather than going directly to the global minimum-energy state.

In the previously studied minimal-aggregation or -fragmentation model,[17] domains of size $(pq)\times(pq)$ are allowed to fragment into p^2 $q\times q$ squares if and only if p is the smallest prime factor of pq. Conversely, a square arrangement of p^2 domains of size $q\times q$ may aggregate to form a $(pq)\times(pq)$ domain if and only if p is the smallest prime factor of pq. Clearly this choice of transition rates maintains ergodic behavior since all configurations are connected to the configuration where every domain is a square of size unity.

The aggregation rate for this model to form a $(pq)\times(pq)$ domain has been chosen as

$$r_a(pq) = \nu_0 \alpha^{2pq(p-1)} \ , \tag{2.3}$$

where ν_0 is a fundamental attempt frequency and α is a rate parameter in the range

$$0 < \alpha < 1 \ . \tag{2.4}$$

The exponent of α in Eq. (2.3) is the length of domain wall which is removed by the aggregation process. Detailed balance then requires that the fragmentation rate be

$$r_f(pq) = r_a(pq)\exp(-\beta\Delta\Phi) \ , \tag{2.5}$$

where

$$\beta = (k_B T)^{-1} \tag{2.6}$$

and

$$\Delta\Phi = 2\lambda pq(p-1) \ . \tag{2.7}$$

In the boundary-shift model a domain of size $(p+1)\times(p+1)$ fragments into a domain of size $p\times p$ and $2p+1$ domains of unit squares. The L-shaped array of unit squares produced by the fragmentation may of course occur in any of four different orientations. Similarly, aggregation occurs when an L-shaped arrangement of unit squares is combined with a domain of size $p\times p$ to form a domain of size $(p+1)\times(p+1)$. Again this choice of transition rates will lead to ergodic behavior since all domain configurations are connected to the configuration where each domain has unit size.

The rate of aggregation for the formation of a domain of size $(p+1)\times(p+1)$ is assigned as

$$r_a = \nu_0 \alpha^{4p} \ , \tag{2.8}$$

where ν_0 and α are as defined previously. The rate of fragmentation of a domain of size $(p+1)\times(p+1)$ then must be

$$r_f(p+1) = r_a(p+1)\exp(-4\beta\lambda p) \ . \tag{2.9}$$

The length of domain boundary which disappears upon aggregation and which forms on fragmentation in both cases is $4p$.

As the temperature is lowered, the equilibrium average size of domains increases in the tiling model. Also the basic transition rates of aggregation in both dynamical models [see Eqs. (2.3) and (2.8)] decrease as the domain sizes increase. In addition, as the domains become larger, it becomes increasingly unlikely that domains of proper geometric arrangement will be found available for aggregation. Therefore both the previous and the present choices for the transition rates produce a kinetic slow-down which will lead to glasslike behavior. Note that the equilibrium properties of the tiling model are independent of which of the two transition options is chosen. Only the kinetic features are affected, and we wish to establish how the relaxation behavior changes in passing from one option to the other.

III. MONTE CARLO SIMULATIONS

The Monte Carlo simulation of any glass presents a formidable problem since as the temperature is lowered toward the glass transition, longer and longer times are required to equilibrate and sample the material adequately. In the standard Monte Carlo formulation due to Metropolis *et al.*,[20] the number of moves which are rejected also increases dramatically at low temperatures which further exacerbates the equilibration problem. To overcome this difficulty a scheme similar to that developed by Bortz, Kalos, and Lebowitz[21] was used in the simulations reported here.

The algorithm is constructed by making a list of all possible aggregation and fragmentation transitions for a given configuration along with their respective transition rates. The total transition rate is then the sum over all of these individual rates

$$R = 1/\Delta t = \sum_{\text{squares}} r_{\square} , \tag{3.1}$$

where Δt is the expected lifetime of the configuration. The Monte Carlo procedure then selects which square to modify and whether the move is a fragmentation or aggregation by chosing a random number between 0 and R. A square is chosen for a change if the partial sum of all previous rates in the list of possible moves is less than the random number and the partial sum of rates including this move is greater than the random number. This algorithm guarantees that every contemplated move is successful. In addition, moves with smaller rates are chosen less frequently because they contribute a smaller fraction to the total rate.

The natural time unit for this problem is $1/\nu_0$, the reciprocal of the fundamental attempt frequency. The rate parameter α which controls the onset of glasslike behavior has been chosen as

$$\alpha = 0.98 \tag{3.2}$$

in both the minimal aggregation model and the boundary-shift model.

Once a move has been made, the list of possible transitions must be modified appropriately. However, only the local environment near the change requires relisting of possible transitions and their rates. Thus only a modest number of transition rates need be modified at each stage of the simulation.

In our previous Monte Carlo simulations of the minimal-aggregation model,[17] we found that the equilibrium results obtained for a system of size of 100×100 ($N=10^4$) were substantially identical to those obtained for a system of size 50×50 ($N=2.5\times10^3$). Therefore only the 50×50 system was studied in the calculations on the boundary-shift model reported here.

The simulations were initiated from a configuration consisting entirely of unit squares at $\beta\lambda=0.10$. This temperature is well above the condensation point (see below) so that the system equilibrated rapidly. Then a long run of over a million moves was made to sample the equilibrium and kinetic properties of the system. The next lower-temperature (higher $\beta\lambda$) run was equilibrated using the end point of the previous sampling run as the starting configuration. Runs were executed in this fashion to a maximum $\beta\lambda$ value of 1.00, which is much lower than the condensation temperature. The run at $\beta\lambda=0.00$ was initiated from the end of the run at $\beta\lambda=0.10$. The run at $\beta\lambda=0.05$ was started from the end of the run at $\beta\lambda=0.00$. Both static and dynamic properties of the tiling model with the boundary-shift transition rates were evaluated at the temperatures of interest by sampling very long runs, typically 4 times longer than the equilibration runs.

IV. ENERGY AND ENTROPY

The average potential energy for various values of $\beta\lambda$ determined from the Monte Carlo simulation of the boundary shift model is listed in Table I. At negative or small values of $\beta\lambda$ the average potential energies determined from both transition-rate models agree within the statistical uncertainties of the simulations. At higher $\beta\lambda$ values, near to but below the condensation point at $(\beta\lambda)_c=0.271$, the current calculations consistently give a lower average potential energy indicating that the boundary-shift transition-rate model does not fall out of equilibrium as rapidly as the other model. Beyond the condensation point both models fall out of equilibrium although in a somewhat different fashion.

We have previously developed a series expansion for the free energy F in the limit $\beta\lambda\rightarrow-\infty$, viz.,

$$\beta F(\beta)/N = 2\beta\lambda - x + \tfrac{9}{2}x^2 - \tfrac{100}{3}x^3 + O(x^4) , \tag{4.1}$$

where

$$x = \exp(4\beta\lambda) . \tag{4.2}$$

It is then easy to show that

$$\langle\Phi\rangle/N\lambda = 2 - 4x + 36x^2 - 400x^3 + O(x^4) . \tag{4.3}$$

A very accurate [3/3] Padé approximant[22] was developed for $\langle\Phi\rangle/N\lambda$ by using the Monte Carlo simulation data of Table I, while simultaneously constraining the Padé coefficients to obey the expansion Eq. (4.3) for small x. The data from the prior minimal-aggregation model from $\beta\lambda=-0.30$ to -0.05 were combined with the data from the boundary-shift model from $\beta\lambda=0.0$ to 0.20, and the three free parameters of the [3/3] Padé approximant were determined using a nonlinear least-squares fit. The following approximant was determined:

$$\frac{\langle\Phi\rangle}{N\lambda} = \frac{2+26.284x+52.000x^2-5.693x^3}{1+15.142x+38.284x^2+1.167x^3} . \tag{4.4}$$

Figure 1 shows the excellent agreement between the simulation data and the [3/3] Padé approximant. The diamonds in the figure are the data points from the simulation of the tiling model using the minimal-aggregation transition-rate rules. The squares are the new points determined using the boundary-shift rules for the transition rates. The poles of Eq. (4.4) all lie on the negative-real axis, at -32.404, -0.316, and -0.0837.

The free energy and entropy of the tiling model may be found from the thermodynamic relationships,

TABLE I. Mean values of the potential energy for the tiling model at various temperatures.

$\beta\lambda$	$\langle\Phi\rangle/N\lambda$[a]	$\langle\Phi\rangle/N\lambda$[b]
−0.30		1.598
−0.20		1.522
−0.10		1.437
−0.05		1.392
0.00	1.340	1.342
0.05	1.286	1.280
0.10	1.225	1.225
0.15	1.157	1.170
0.20	1.076	1.092
0.25	0.964	1.015
0.268	0.920	
0.30	0.848	0.890
0.35	0.707	0.716
0.40	0.576	0.593
0.45	0.511	0.486
0.50	0.472	0.440
1.00	0.433	0.409
10.00		0.405

[a]Results using the boundary-shift transition-rate rules, Eqs. (2.8) and (2.9).
[b]Results using the minimal-aggregation transition-rate rules, Eqs. (2.3)–(2.7).

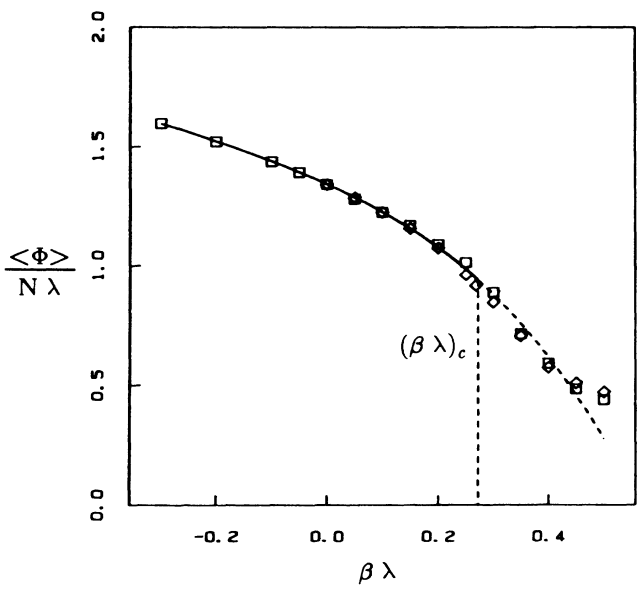

FIG. 1. Comparison of the Monte Carlo simulation data for the square-tiling model with the Padé approximate (solid curve) given in Eq. (4.4). The transition rate rules using the minimal-aggregation model are plotted as squares, and using the boundary-shift model are plotted as diamonds. Both models are in excellent agreement with each other and the Padé method at temperatures above the condensation point, $(\beta\lambda)_c$ to the left of the dashed line. The Padé result and both models differ significantly below the condensation temperature.

$$\frac{\beta F}{N}=2\beta\lambda+\int_{-\infty}^{\beta\lambda}\left[\frac{\langle\Phi\rangle}{N\lambda'}-2\right]d(\beta\lambda)' \tag{4.5}$$

and

$$\frac{S}{k_B N}=-\frac{\beta F}{N}+\beta\lambda\left[\frac{\langle\Phi\rangle}{N\lambda}\right] . \tag{4.6}$$

Equation (4.5) was integrated numerically using the Padé approximant of Eq. (4.4) to determine the free energy. Figure 2 shows the result as a function of $\beta\lambda$. The free energy is a monotonically increasing function of $\beta\lambda$ in the range shown, and goes to zero at the condensation point: $(\beta\lambda)_c=0.271$. This value had been estimated previously to be 0.268 from the simulations of the tiling model using the minimal-aggregation transition rate rules.

The entropy of the model as a function of $\beta\lambda$ is shown in Fig. 3. The total number of square tilings is given by the entropy at infinite temperature, i.e., $\beta\lambda=0$ and is thereby found to be

$$\Omega_{\text{tot}}=\exp(0.3156N) . \tag{4.7}$$

This is in excellent agreement with the previously calculated value.

We have analytically shown previously that at temperatures above the condensation point, the equilibrium concentration of domains of size $j\times j$ monotonically decreases with size and in addition that the concentration to good approximation obeys the following equation:

$$\ln(n_j/N)=-Kj^2-Lj-M . \tag{4.8}$$

At temperatures higher than the condensation temperature the parameters K and L are both positive and refer, respectively, to the interior and the boundary free energy

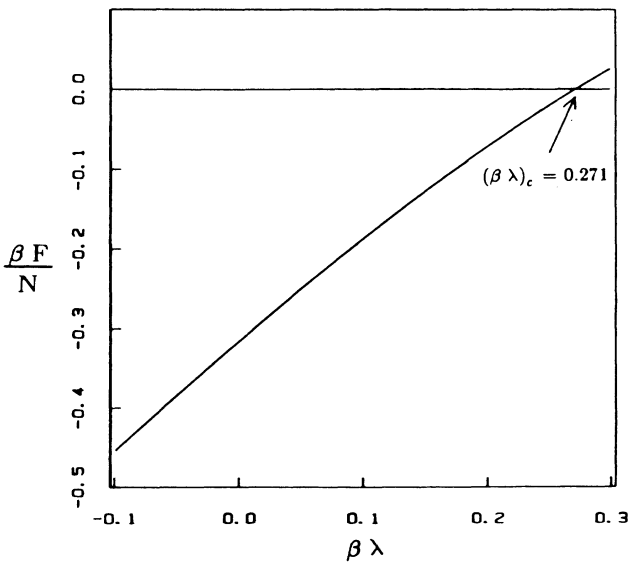

FIG. 2. The free energy for the square-tiling model [Eqs. (4.4) and (4.5)] as a function of $\beta\lambda$. The free energy vanishes at $(\beta\lambda)_c=0.271$.

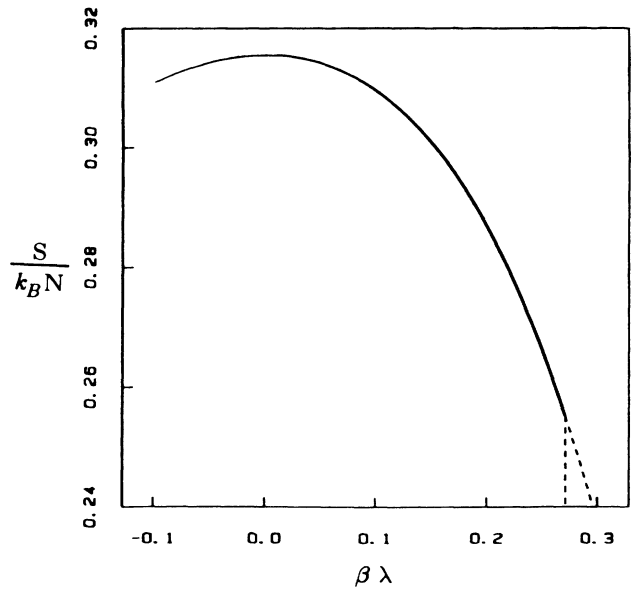

FIG. 3. The entropy for the square-tiling model [Eqs. (4.4)–(4.6)] as a function of $\beta\lambda$.

for the medium in which the $j \times j$ domain is inserted.

The average concentrations of domains as determined from the computer simulations were fitted by least squares to Eq. (4.8). Figure 4 shows a plot of the logarithm of the domain concentration versus the domain edge length at $\beta\lambda = 0.2$, and the fitting function so determined. Because of the small number of largest sized domains, and therefore the uncertainty in their average concentration, that value was not used in the least-squares fit. The coefficients K, L, and M determined from the fits as a function of $\beta\lambda$ are given in Table II.

TABLE II. $\ln c(l) = -Kl^2 - Ll - M$.

$\beta\lambda$	K	L	M
0.00	0.304	0.398	0.211
0.05	0.223	0.615	0.146
0.10	0.160	0.727	0.211
0.15	0.116	0.771	0.352
0.20	0.073	0.814	0.523
0.25	0.023	0.917	0.686
0.268	−0.006	1.034	0.660
0.30	−0.036	1.117	0.760
0.35	−0.069	1.174	1.107
0.40	−0.101	1.251	1.507
0.45	−0.099	1.154	1.958
0.50	−0.078	0.918	2.562
1.00	0.001	0.176	4.081

As expected the leading coefficient K decreases monotonically as the temperature is lowered toward the condensation point. Very close to the value of $(\beta\lambda)_c$ determined from the free energy, we see that K becomes 0 (Fig. 5).

There is excellent agreement between the values for the number of tilings at infinite temperature as estimated for the two kinetic models for the transition rates. This further supports our previous conclusion of a first-order thermodynamic phase transition for the tiling model at $(\beta\lambda)_c$, providing strict equilibration obtains. The main interest in both kinetic versions of the tiling model concerns the failure to achieve equilibration at and below the condensation point.

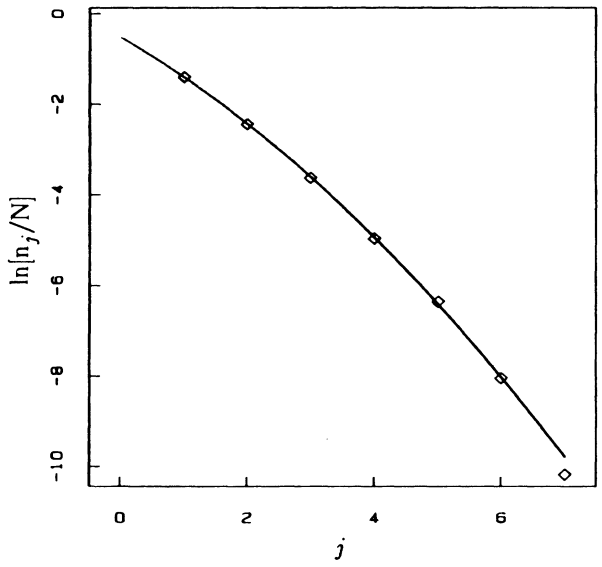

FIG. 4. The logarithm of the concentration of $j \times j$ squares as a function of j at temperature $\beta\lambda = 0.2$. The solid curve is a least-squares fit of the data, excluding the last point, to Eq. (4.8).

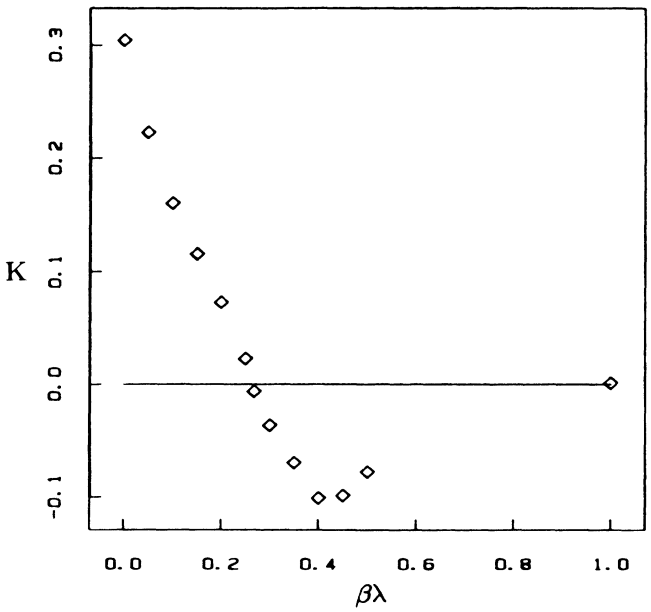

FIG. 5. A plot of the area coefficient K as a function of $\beta\lambda$, see Eq. (4.8). An estimate of the condensation temperature is given by the point at which K goes to zero.

V. RELAXATION RATES

The high-temperature equilibrium properties of the square-tiling model are in substantial agreement for both transition rate models. However, the dynamical properties of the two models are expected to differ significantly depending upon the choice of transition rate rules. In an attempt to investigate the linear dynamical response, we have evaluated the potential energy autocorrelation function, defined by

$$\phi(t)=\frac{\langle\Phi(t)\Phi(0)\rangle-\langle\Phi\rangle^2}{\langle\Phi^2\rangle-\langle\Phi\rangle^2}\ . \tag{5.1}$$

For the minimal aggregation model, we found that only the short-to-intermediate-time decay for values of $\beta\lambda\leq 0.1$ could be obtained with reasonable accuracy. For the boundary-shift model, we have been able to extend the temperature range closer to the condensation temperature, and still accurately calculate the relaxation behavior. Using the Monte Carlo simulation data from the long equilibrium runs, we have calculated the autocorrelation function Eq. (5.1) from the chain of configurations saved at various times.

The resulting numerical autocorrelation functions were then fitted to the Kohlrauch-Williams-Watts (KWW) function[23]

$$\phi(t)=\exp[-(t/\tau_\omega)^\mu]\ , \tag{5.2}$$

where τ_ω and μ are the adjustable parameters determined by a nonlinear least-squares fit to the data. Figure 6 shows the autocorrelation function obtained from the simulation and the KWW fit to the data at $\beta\lambda=0.05$. Figure 7 shows a similar plot for a lower-temperature run at $\beta\lambda=0.20$. In both cases the KWW fit is in good agreement with the data. However the μ parameters differ substantially, 0.560 and 0.401, respectively, indicating not only that a single exponential would not have yielded a good fit, but that the discrepancy magnifies as temperature declines.

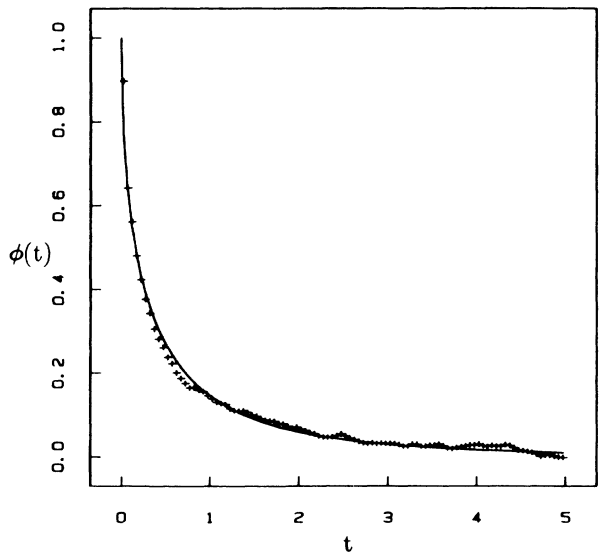

FIG. 6. A plot of the potential-energy autocorrelation function, Eq. (5.1), vs time for $\beta\lambda=0.05$. The solid curve is a fit to the data using the KWW function, Eq. (5.2).

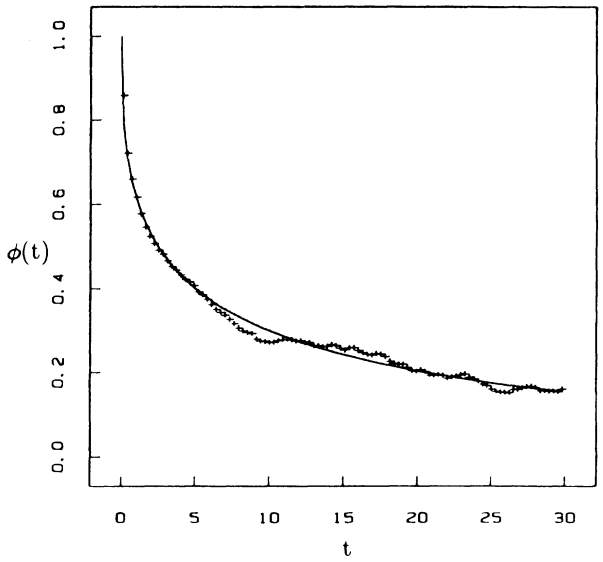

FIG. 7. A plot of the potential-energy autocorrelation function, Eq. (5.1), vs time for $\beta\lambda=0.20$. The solid curve is a fit to the data using the KWW function, Eq. (5.2).

The values of the KWW parameters obtained from the fits are listed in Table III. Due to the uncertainties in the autocorrelation-function data obtained from the simulations and in the least-squares fits themselves, the average relaxation time defined by

$$\langle\tau\rangle=\int_0^\infty \exp[-(t/\tau_\omega)^\mu]dt=\tau_\omega\mu^{-1}\Gamma(\mu^{-1}) \tag{5.3}$$

has been our preferred method to compare relaxation rates as a function of temperature. The average relaxation times calculated for both transition rate models are also listed in Table III. It is immediately evident that the boundary shift model relaxes more quickly, a factor of 4 times faster at $\beta\lambda=0$, than the minimal aggregation model.

Figure 8 shows an Arrhenius plot of the logarithm of

TABLE III. Values of the average relaxation time as a function of temperature.

$\beta\lambda$	τ_ω	μ	$\langle\tau\rangle^a$	$\langle\tau\rangle^b$
0.00	0.145	0.804	0.164	0.65
0.05	0.309	0.560	0.512	1.5
0.10	0.660	0.571	1.064	5.6
0.15	1.532	0.521	2.848	
0.20	6.223	0.401	20.600	
0.25	22.169	0.638	30.925	
0.268	48.161	0.354	295.200	

[a]Results using the boundary-shift transition-rate rules, Eqs. (2.8) and (2.9).

[b]Results using the minimal-aggregation transition-rate rules, Eqs. (2.3)–(2.7).

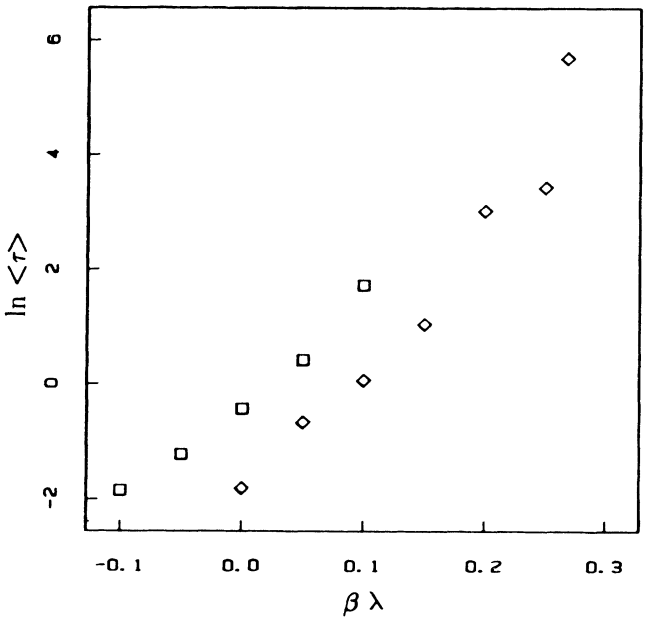

FIG. 8. An Arrhenius plot of the average relaxation time [Eq. (5.3)] for the potential energy. The diamonds are the new data obtained using the boundary-shift model. The squares are the data of the minimal-aggregation model. The slope or activation energy increases as the temperature is lowered ($\beta\lambda$ increased).

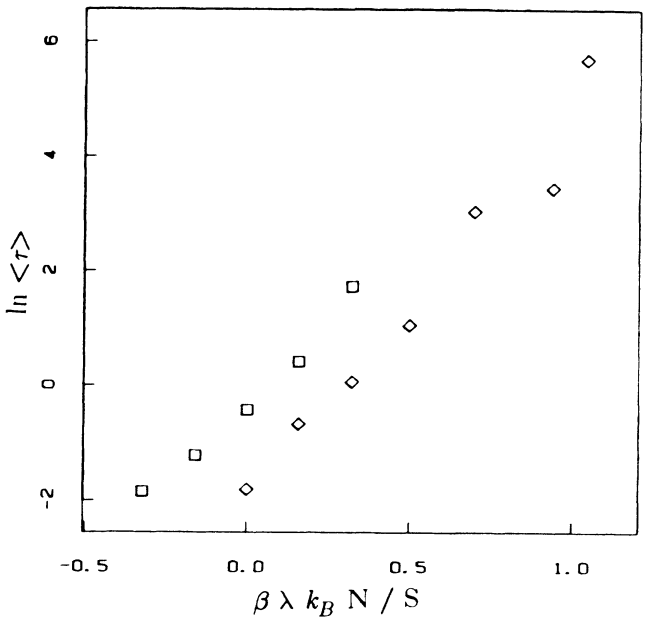

FIG. 9. Adam-Gibbs correlation for the square-tiling model. The diamonds are the new data obtained from simulation using the boundary-shift model. The squares are the data from the minimal-aggregation model.

the average relaxation time for the boundary-shift transition-rate version of the square-tiling model. The apparent energy of activation is seen to increase as the temperature decreases toward the condensation temperature, as would be expected for a material approaching its glass transition.[1,24] Previously we had investigated whether the properties of the square-tiling model obeyed the Adam-Gibbs hypothesis,[2] viz., the energy of activation is inversely proportional to the entropy. Figure 9 shows a plot of $\ln\langle\tau\rangle$ versus $\beta\lambda k_B N/S$. As with the minimal aggregation model, the apparent curvature in the present plot (Fig. 9) indicates that the kinetics of the boundary shift model do not strictly obey the Adam-Gibbs equation.

VI. DISCUSSION

Both the minimal-aggregation and the boundary-shift models rapidly approach equilibrium at temperatures well above the condensation temperature. However, as the temperature is lowered through the condensation temperature the minimal-aggregation model falls out of equilibrium sooner than the boundary-shift model. At temperatures much lower than the condensation temperature the minimal-aggregation model has a lower average potential energy implying a closer approach to equilibrium although both models are still far from equilibrium.

The ability to reach equilibrium in the square-tiling model is inherent in the basic kinetic assumptions used respectively for the two cases. At high to moderate temperatures where the number of unit squares is substantial, larger squares may form by aggregation using either set of transition rate rules. Thus the concentrations of domains of size greater than unity will attain their equilibrium values readily.

As the temperature is lowered toward the condensation temperature, the concentration of unit squares decreases. The formation of larger squares in the boundary-shift mode is then slowed because of the lack of unit squares in the proper arrangement to aggregate with existing domains. In this kinetic version, unit squares must be created by the fragmentation of neighboring domains which can then aggregate with another domain to form a larger domain. Equilibrium concentrations of larger domains may only be obtained by fragmentation processes followed by aggregation.

However, with the minimal-aggregation-model transition-rate rules, tilings may eliminate boundaries whenever any domains of the same size find themselves in a square arrangement. Thus four large squares in proper registry may form a still larger square. This process can still occur even at the lowest temperatures provided the concentrations of domains of the same size are great enough. Thus the minimal-aggregation model may be able to lower its average potential energy at very low temperatures while the boundary-shift model is unable to lower its energy because of the low concentration of unit squares in proper alignment.

Not surprisingly, perhaps, we find that the patterns, or textures, of square tiles in the low-temperature glasses produced with the two kinetic alternatives are subtly different. With the minimal-aggregation rules, significant collineations of unit squares become trapped

in the matrix of large squares. These are substantially absent in the glasses formed with incremental aggregation. In addition, tiles of the prime-number size 7×7 form with greater difficulty (and so appear in lower concentration) with the minimal aggregation rules in comparison with incremental aggregation rules. If computing resources were available to cool several orders of magnitude more slowly than thus far possible, we expect that even larger prime-number squares ($11\times11, 13\times13$, ...) would be observed with incremental domain kinetics, whereas the one-step formation of these prime-number tiles required by the minimal kinetics would be extremely unlikely.

The kinetics of both models have been fitted empirically with the KWW functional form. This function has been found to adequately model the short to moderate time relaxational behavior of the square-tiling model. We have shown that the very-long-time relaxational behavior of the KWW functional form decays to zero faster than the true relaxational behavior.[17] Similar arguments may be applied to the boundary shift model to show that the KWW form, though certainly useful as a fitting tool, does not possess the correct very-long-time behavior.

Both kinetic variants have been shown to have non-Arrhenius behavior. The activation energy increases as the temperature is lowered as would be expected for a material approaching a glass transition. In addition, the Adam-Gibbs hypothesis[2] is found not to be accurately obeyed in both the minimal-aggregation and boundary-shift cases.

One of the distinctive features of the square-tiling models is the ability to define a coherence length which may be associated with the size of a tile. This length should diverge as the temperature is lowered if equilibrium is achievable, as the tiles grow to encompass the entire sample; however, it does not because the glass transition intervenes.

There are many possible variants of the transition rate rules which could be used to study the square-tiling model. The two studied to date represent opposite geometric extremes of possible aggregation and fragmentation. Both show a failure to reach equilibrium as the temperature is lowered through the transition temperature. However the rates at which, and the extents by which, the tiling model falls out of equilibrium depend significantly on the allowed set of fundamental transitions. Furthermore, the final spatial patterns of domains in the glass as temperature goes to zero likewise depend on the allowed set of transitions in subtle ways not explainable by a simple shift in effective time scales.

We conclude that it will be valuable to expand the range of kinetic models and sets of allowed transitions to sharpen general understanding of these complex effects.

[1]H. Rawson, *Properties and Applications of Glasses* (Elsevier, Amsterdam, 1980).
[2]G. Adam and J. H. Gibbs, J. Chem. Phys. **43**, 139 (1965).
[3]M. H. Cohen and G. S. Grest, Phys. Rev. B **20**, 1077 (1979); **21**, 4113 (1980).
[4]E. Leutheusser, Phys. Rev. A **29**, 2765 (1984).
[5]S. P. Das, G. F. Mazenko, S. Ramaswamy, and J. J. Toner, Phys. Rev. Lett. **54**, 118 (1985).
[6]T. R. Kirkpatrick, Phys. Rev. A **31**, 939 (1985).
[7]J. J. Ullo and S. Yip, Phys. Rev. Lett. **54**, 1509 (1985).
[8]U. Bengtzelius, W. Goetze, and A. Sjolander, J. Phys. C **17**, 5915 (1984).
[9]G. H. Fredrickson and H. C. Andersen, Phys. Rev. Lett. **53**, 1244 (1984).
[10]G. H. Fredrickson and H. C. Andersen, J. Chem. Phys. **83**, 5822 (1985).
[11]G. H. Fredrickson and S. A. Brawer, J. Chem. Phys. **84**, 3351 (1986).
[12]O. S. Narayanaswamy, J. Am. Ceram. Soc. **54**, 491 (1971).
[13]C. T. Moynihan, P. B. Macedo, C. J. Montrose, P. K. Gupta, M. A. DeBill, B. E. Dow, P. W. Drake, A. J. Easteal, P. B. Elterman, R. P. Moeller, H. Sasabe, and J. A. Wilder, Ann. N.Y. Acad. Sci. **279**, 15 (1976).
[14]A. J. Kovacs, Ann. N.Y. Acad. Sci. **371**, 21 (1981).
[15]G. W. Scherer, J. Am. Ceram. Soc. **67**, 504 (1984).
[16]F. H. Stillinger and T. A. Weber, Ann. N.Y. Acad. Sci. **484**, 1 (1986).
[17]T. A. Weber, G. H. Fredrickson, and F. H. Stillinger, Phys. Rev. B **34**, 7641 (1986).
[18]F. H. Stillinger and T. A. Weber, Science **225**, 938 (1984).
[19]F. H. Stillinger and R. A. LaViolette, Phys. Rev. B **34**, 5136 (1986).
[20]N. Metropolis, A. W. Metropolis, M. N. Rosenbluth, A. H. Teller, and E. Teller, J. Chem. Phys. **21**, 1087 (1953).
[21]A. B. Bortz, M. H. Kalos, and J. L. Lebowitz, J. Comput. Phys. **17**, 10 (1975).
[22]G. A. Baker, Jr., J. L. Gammel, and J. G. Wills, J. Math. Anal. Appl. **2**, 21 (1961); **2**, 405 (1961).
[23]A. K. Jonscher, Nature (London) **267**, 673 (1977).
[24]S. Brawer, J. Chem. Phys. **81**, 954 (1984).